ORIGINAL ARTICLE

Muscle Thickness Measurement from Reflection Echo of the Boundary Surface

Saadia Binte Alam*

Graduate School of Engineering, University of Hyogo, Japan, and
Department of Electrical and Electronics Engineering, International University of Business Agriculture and Technology,Bangladesh

Rashedur Rahman

Department of Electrical and Electronics Engineering, International University of Business Agriculture and Technology,Bangladesh

Manabu Nii

Graduate School of Engineering, University of Hyogo, Japan

Syoji Kobashi

Graduate School of Engineering, University of Hyogo, Japan

Yutaka Hata, *Fellow, IEEE*

Graduate School of Simulation Studies, University of Hyogo, Japan

Abstract

The loss of muscle mass is considered to be a major determinant of strength loss among elderly population. A study of muscular thickness measurement method founded on reflection echo from the boundary surface of the targeted area using ultrasonic wave is presented. By exploring the traveling direction of ultrasonic wave at the boundary surface of fat-muscle or muscle-fat, phase difference of the generated reflection echo can be measured. In the present study, boundary surface is identified by utilizing the difference of the reflected echo at frontier surface. Two different methods of interface echo recognition are introduced. To measure the reflection echo, ultrasonic waves are irradiated to a biological phantom using ultrasonic single probe with center frequency of 5.0 MHz. In an experimental environment, the proposed methods were applied to a fat-muscle-fat 3-layer phantom and muscle thickness was measured. In the template based method, the mean absolute error of the thickness was 0.32 mm, whereas for continuous wavelet transform (CWT) based method was 0.06 mm. It was observed that the level of the measurement precision is better in the CWT based method.

Keywords: Ultrasonic wave, boundary surface, reflection echo, muscle thickness, CWT, Complex Gaussian wavelet.

1. INTRODUCTION

Muscle weakness is consistently reported as an independent risk factor for high mortality in older adults [1].

The loss of muscle mass is considered to be a major determinant of strength loss in aging population. Since muscle strength appears to be a critical component in maintaining physical function, mobility, and vitality in old age, it is paramount to quantify the loss of strength in elderly persons [2]. Recent muscle mass estimation method uses a body composition monitor which is designed for home use. However, its reliability is low because it estimates mass using a body fat percentage based on bio-electrical impedance and body weight. Thus, this body composition meter is not suitable for local measurement, such as

---

*Corresponding author
  Email addresses:* saadiabinte@ieee.org (Saadia Binte Alam),
rashed.riyadh14@gmail.com (Rashedur Rahman),
nii@eng.u-hyogo.ac.jp (Manabu Nii),
kobashi@eng.u-hyogo.ac.jp (Syoji Kobashi), hata@ieee.org
(Yutaka Hata)

the measurement of thigh muscle mass. Therefore, in this study, we used an ultrasonic device which is capable of local measurement, compact, low cost, and that also had the advantage of portability. In order to improve the accuracy of the muscle mass measurement, it is necessary to divide the area of fat and muscle to be distributed in the body.In [3], region of muscle and fat was extracted from the ultrasonic waveform, which utilized acoustic velocity change in the medium according to temperature changes. In the human body, the speed of sound increases with temperature rise in the muscle, however, it decreases in the fat. The method is based on the echo reflected from the medium boundary, it divides the medium portion into two. This method assumes that the measurement result of before and after temperature rise is essential, and measurement conditions need to be totally same other than temperature, and also, the thickness of the measurement point is limited to one point. Further, when applied to the human body, raise the temperature of the measuring part uniformly is extremely difficult. That is why, the fat and muscle distinguishable technique has been required without using the parameter of temperature change.

This study aims to identify the reflection echo from the boundary surface of the targeted area in order to acquire muscle thickness. When the ultrasonic wave reaches the mediums boundary surface, reflection echo occurs due to acoustic impedance change. By exploring the traveling direction of ultrasound at the boundary surface of fat-muscle or muscle-fat, phase difference of the generated reflection echo can be measured. In the present study, boundary surface is identified by utilizing the difference of the reflected echo at frontier surface. Two different methods of interface echo recognition are introduced. To measure the reflection echo, ultrasonic wave irradiated to a biological phantom using ultrasonic single probe with center frequency of 5.0 MHz. In an experimental environment, the proposed methods were applied to a fat-muscle-fat 3-layer phantom, where we distinguish the two types of boundaries mentioned above, and estimate the thickness of the muscle using two different approaches.

2. PRELIMINARY

2.1. Data acquisition

The ultrasonic data acquisition system used in this experiment is shown in Fig. 1. In this system, ultrasonic wave was irradiated from the ultrasonic single probe to a biological phantom. Temperature of the biological phantom was controlled at 36 °C by using a thermometer. The reflected wave was transferred into the computing system through pulse receiver, and the AD converter (Pico Technology, Scope 4227). It should be noted that, the sampling interval of the data was set to 4 ns. Ultrasonic single probe used in the present study is shown in Fig. 2. As the propagation range of the measurement target becomes smaller, the spatial resolution becomes high and vice versa.

In this study, the ultrasonic probe [4,5] with a wavelength of 300 μm at 5.0 MHz was applied. For experiment purpose, four measurements of ultrasonic wave were acquired. Each measurement contained 5 individual acquisition of the same phantom.
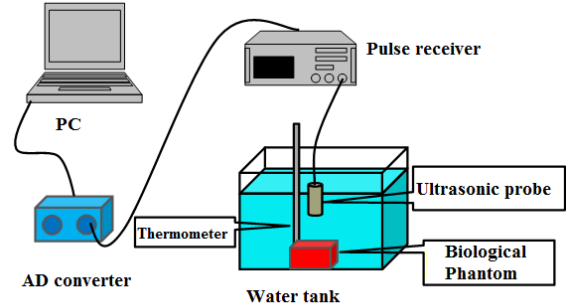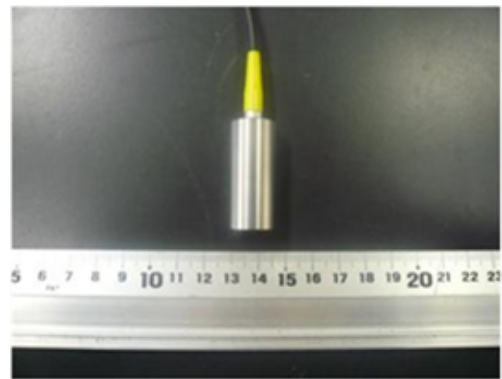

Figure 1: Ultrasonic data acquisition system

Figure 2: Ultrasonic single probe

2.2. Interface echo

A part of the irradiated ultrasonic wave from the ultrasonic probe is reflected at the interface of each different media. By receiving the reflected echo using ultrasonic probe, we can measure a large voltage magnitude in the waveform. In this paper, reflection echo obtained from the medium boundary surface is called interface echo. Proposed method first identifies the medium interface by detecting the interface echo with two different approaches and then perform thickness measurement.

When irradiated ultrasonic waves reach the medium interface, we measure interface echo from two different perspectives: fat comes first then muscle, or muscle comes first then fat. Afterwords, interface echo occurrence difference depending on the order of the medium is investigated. It should be noted that, in this paper, interface echo that occurs when it reaches from the fat to muscle referred as interface echo A, and interface echo that occurs when it

reaches from muscle to fat as interface echo B. Fig. 3 indicates the fat phantom and muscle phantoms used for this specific study.
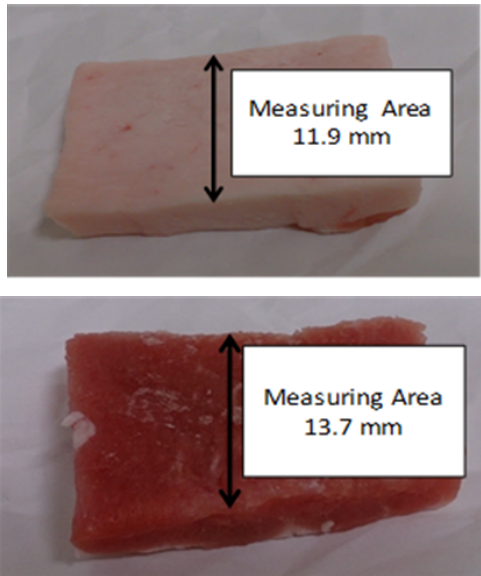

Figure 3: Biological phantom. Fat phantom (top), Muscle phantom (bottom)

Figure 4: Measurement result of interface echo A. Waveform measurement (top), Magnification of the interface (bottom)

For experimental setup, two phantoms were vertically laid one on the other and fixed. Then, ultrasonic waveform was acquired by irradiating ultrasonic wave from the top of the stacked biological phantom. An example of the result where the fat surface comes on the top is shown in Fig. 4, and an example of the result where the muscle surface comes on the top is shown in Fig. 5. From the measurement waveform of in Fig. 4, the voltage amplitude of the interface echoes A shows positive direction at the beginning of the amplitude. On the other hand, from the measurement waveform of Fig. 5, the voltage amplitude of the interface echo B shows negative direction at the beginning of the amplitude. From these results, it is documented that phase inversion takes place between interface echo A and B.

3. Proposed Method

The present study deals with two different methods of muscle thickness measurement. First method is based on interface echo template and the second one uses continuous wavelet transformation (CWT). The details are stated bellow.

3.1. Template based method

The methodology combines: i) Template creation from interface echo; ii) Threshold processing; iii) Template matching; iv) Boundary surface identification; v) Thickness measurement. Details are given bellow.
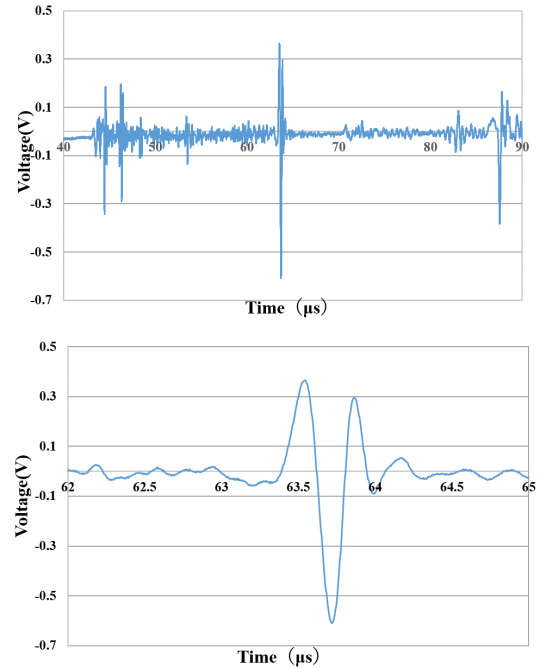
3.1.1. Template creation

In the first step, we create templates with characteristics of interface echo A and B. As a creation method, first, the ultrasonic measurement at a plurality of measurement points are performed with the fat surface up of the superimposed biological phantom, and it obtains the ultrasonic waveform at each measurement point following data extraction of interface echo A form the acquired ultrasonic waveform. By means of detecting the point where the voltage value crosses zero just before the first amplitude starts in the voltage amplitude of the interface echo A, a point before 0.2 μs is set as the starting point of the extraction range, and a point after 0.8 μs is set as the end point of the extraction range. Then, the range from the start point to the end point of the interface echo A is mined as the data. Similarly, ultrasonic measurement is performed at a plurality of measurement points with the muscle surface up, and the data of the interface echo B in each measurement is extracted. Next, the data of the extracted interface echo A, and the data of B, are averaged for each data, and these are the templates of interface echoes. Fig. 6 shows the template of interface echo which was created. In addition, as a result of calculating the correlation coefficients with the two templates, it became clear that there is a strong negative correlation with -0.7613.

3.1.2. Threshold processing

A large voltage amplitude is generated by receiving interface echo with the ultrasonic probe. In this feature, threshold processing by using standard deviation is pro-
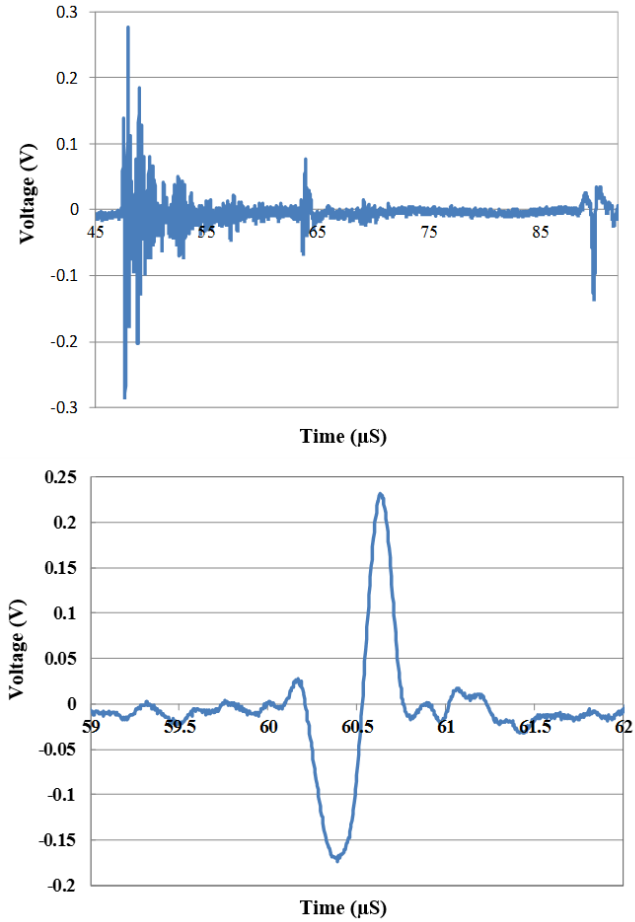
Figure 5: Measurement result of interface echo B. Waveform measurement (top), Magnification of the interface (bottom)

Figure 6: Template of interface echo A (top), Template of interface echo B (bottom)

posed as the first step of narrowing down of boundary surfaces. A schematic diagram of threshold processing is shown in Fig. 7. First, ultrasonic waves are irradiated from the ultrasonic single probe to the object to be measured, and an ultrasonic waveform is acquired. Next, as shown in Eq. (1), the standard deviation σ_{th} of the whole obtained waveform is calculated, and this numerical value is set as the threshold value.

$$\sigma_{th} = \sqrt{\frac{1}{M} \sum_{i=1}^{M} (v(i) - \bar{v})^2} \qquad (1)$$

here, M is the data length of the acquired waveform, and $v(i)$ is the received voltage value at the point i. Next, the partial standard deviation, $\sigma(S)$ of the received voltage from the point S to the point $S + N - 1$ is calculated as shown in the Eq. (2). The length of N is the same as the template of interface echo.

$$\sigma(S) = \sqrt{\frac{1}{N} \sum_{i=S}^{S+N-1} (v(i) - \bar{v}_s)^2}, 1 \leq S \leq M - N + 1 \quad (2)$$
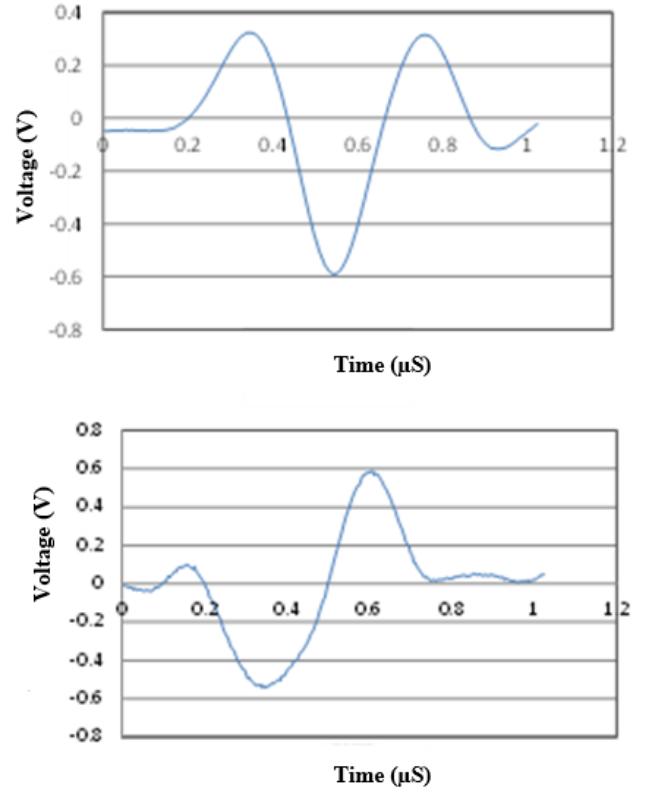
where, $\bar{v}_s$ is the average value of the received voltages from point S to point $S + N - 1$. When the calculated standard deviation $\sigma(S)$ is larger than the threshold σ_{th}, the point S becomes a slate point of a boundary surface. The above threshold processing is performed within the range of S, and all the points S where the deviation is larger than the threshold values were acquired as slate points of the boundary surface.

In this paper, the first reflected wave is generated when it reaches the phantom surface from the water in the tank, and the last reflected wave is generated when it reached to the boundary surface of the bottom of the water tank from the bottom of the phantom. Thus, the first and last voltage amplitude groups do not correspond to either interface echo of A or B. Therefore, in the first voltage amplitude group when the standard deviation exceeds the threshold, the first point where the standard deviation exceeds the threshold is regarded as the phantom surface point, and the time T_f is acquired. Then, among the last voltage amplitude groups exceeding the threshold value, the first point that the standard deviation exceeds the threshold value regarded as a phantom bottom surface point and the time T_e is acquired. After that, the first and last voltage amplitude groups are excluded from candidates of interface echoes A and B. Finally, at the slate point S of interface
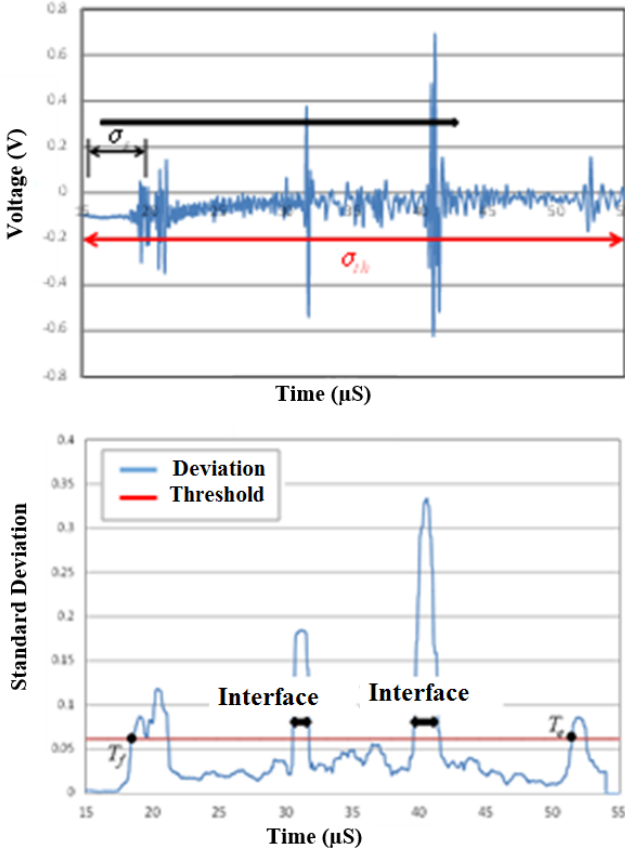
Figure 7: Schematic diagram of threshold processing, Measurement wave pattern (top), and Standard deviation (bottom)

echoes A and B, the received voltage value from the point S to the point $S + N - 1$ is acquired as $\bar{v}_s$.

3.1.3. Template matching

Template matching is performed on boundary surface candidates specified by threshold processing. The template which is applied here means the template of interface echoes of A and B created in section 3.1.1. The correlation coefficient $R_A(S)$ between the interface echo A and point S, and the correlation coefficient $R_B(S)$ between the interface echo B and point S are calculated by Eq. (3) and Eq. (4).

$$R_A(S) = \frac{\sum_{i=1}^{N}(v_s(i) - \bar{v}_s)((v_A(i) - \bar{v_A}))}{(\sqrt{\sum_{i=1}^{N}\{v_s(i) - \bar{v}_s\}}\sqrt{((v_A(i) - \bar{v_A})))}} \quad (3)$$

$$R_B(S) = \frac{(\sum_{i=1}^{N}(v_s(i) - \bar{v}_s)((v_B(i) - \bar{v_B})))}{(\sqrt{\sum_{i=1}^{N}(v_s(i) - \bar{v}_s)}\sqrt{((v_B(i) - \bar{v_B}))}} \quad (4)$$

where, $v_A(i)$ is the voltage value of the template of interface echo A, $\bar{v_A}$ is its average value, $v_B(i)$ is the voltage value of the template of interface echo B, and $\bar{v_B}$ is its average value.
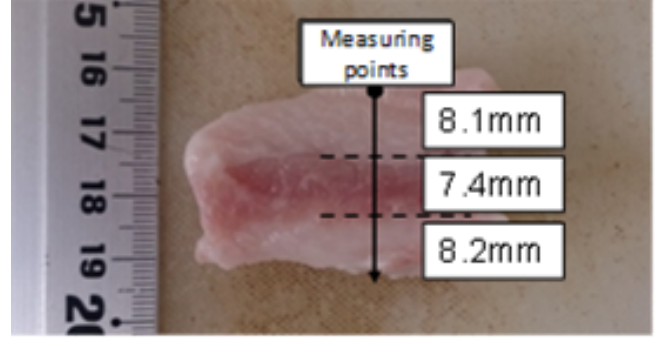

Figure 8: Three layers biological phantom

3.1.4. Boundary surface identification

From the result obtained by template matching, further narrowing down is carried out to specify the boundary surface. At the point S, when there is a strong positive correlation in the template of the interface echo A, and also, there is a strong negative correlation in the template of the interface echo B, that point is the point where the interface echo A occurs. Also, if there is a strong positive correlation in the template of the interface echo B, and also there is a strong negative correlation in the template of the interface echo A, that point is the point where the interface echo B occurs. Next, structural features of the measurement object are used. In this paper, fat and muscle regions are assumed to be distributed alternately. From this, it can be defined that the interface echo A occurs at the odd numbered boundary surface and the interface echo B occurs at the even numbered boundary surface within the region from the phantom surface to the bottom surface. From the above characteristics, in the medium, time T_i at which the i_{th} interface echo A, or the interface echo B occurrence can be narrowed down as in Eq.(5).

$$T_i = t(S); \text{if } R_A(S) > R_{th} \,\&\, R_B(S) > -R_{th}\,\&\, i = 2n - 1$$
$$T_i = t(S); \text{if } R_B(S) > R_{th} \,\&\, R_A(S) > -R_{th}\,\&\, i = 2n$$
$$(5)$$

here, n is an integer, $t(S)$ is the time at point S, and R_{th} is the threshold value of the correlation coefficients. R_{th} is defined as 0.6 from the result of the template matching. By performing the above processing, it is possible to detect the time when the interface echo A, and B will occur.

3.1.5. Thickness measurement

At first, the region is divided from the medium of interface boundary arrival time of the ultrasonic wave which is specified by the narrowing down process followed by the specification of medium of each divided region. The interface echo A is a reflected wave generated when the ultrasonic wave reaches the fat-muscle interface. From this, the area, before the time at which the interface echo A occurs, corresponds to fat, and the area, after the time at which the interface echo A occurs, corresponds to the muscle.

On the other hand, the interface echo B is a reflected wave generated when the ultrasonic wave reaches the muscle-fat interface. Thus, the area, before the time at which the interface echo B occurs, corresponds to muscle, and the area after the time at which the interface echo B occurs, corresponds to fat.

Next, the ultrasonic wave propagation time D_i, is calculated in the divided area of fat and muscle by Eq.(6), where k number of interface echoes A or interface echoes B are detected.

$$D_i = \begin{cases} T_i - T_f; & \text{if } i = 1 \\ T_i - T_{i-1}; & \text{if } 2 \le i \le k \\ T_e - T_{i-1}; & \text{otherwise} \end{cases} \quad (6)$$

By multiplying the propagation time with the sound velocity in the medium from the Eq. (6), the thickness of the fat layer, and the thickness of the muscle layer of the biological phantom L_i, are calculated [6].

$$L_i = \begin{cases} V_F \frac{D_i}{2}; & \text{if } i = 2n - 1 \\ V_M \frac{D_i}{2}; & \text{if } i = 2n \end{cases} \quad (7)$$

where, n indicates an integer, V_F indicates the sound speed in the fat, and V_M indicates the sound speed in the muscle. In this paper, the temperature of the biological phantom is set to 36° C, and the V_F at that time is 1420 m/s, and the V_M is 1566 m/s [7].

3.2. CWT based method

This method is an automated approach of interface echo identification along with muscle thickness measurement. The details are stated bellow.

3.2.1. CWT analysis

A wavelet transform is defined in terms of basis functions obtained by the compression/dilation and shifting of a mother wavelet. In the CWT, the analyzing function is a mother wavelet, ψ [8]. The CWT compares the signal to shifted and compressed or stretched versions of a mother wavelet. Stretching or compressing a function is collectively referred as scaling and corresponds to the physical notion of scale. By comparing the signal to the mother wavelet at various scales and positions, we obtain a function of two variables, scale and position. The generalized CWT function [9] of scale and position for a scale parameter, $a > 0$, and position, b, is:

$$CWT_n^\psi(a,b) = \int x(t)\psi_{a,b}^*(t)dt \quad (8)$$

We can include that not only the values of scale and position affect the CWT coefficients but also the choice of wavelet affects the values of the coefficients. Numerous wavelet bases with different features are found in the wavelet transform, and appropriately choosing among these

bases is important because different features may produce varying results for the same signal [10]. Experiments in which different wavelet bases are conducted in the present study and upon careful consideration, the complex Gaussian wavelet is chosen as the basis for analyzing phase synchronization. Complex-valued wavelets are useful in cases where it is necessary to analyze phase as well as magnitude. A Gaussian function is one of the best window function for time-frequency location and is widely used in signal analysis and processing. Complex Gaussian wavelet is built from the complex Gaussian function $f(x) = C_q e^{-x^2} e^{-ix}$ while taking the qth derivative of f. In this equation, q is the integer parameter and C_q can be written such that $||f^{(q)}||^2 = 1$; where $f^{(q)}$ is the qth derivative of f.

3.2.2. Local maxima detection

Complex Gaussian wavelet of 4th order is applied on the extracted signal. From the result, local maxima are detected. Then, an envelop curve is created which connects signal values of local maxima. For two consecutive local maxima L_1 and L_2, the envelop curve was calculated by the following equation

$$\alpha_1 = y_1 + \frac{y_2 - y_1}{t_2 - t_1} \quad (9)$$

where, y_1 is the signal value of L_1, y_2 gives signal value of L_2, t_1 corresponds time of L_1, and t_2 gives time of L_2. Finally, the signal can be represented as

$$f(\alpha) = [\alpha_1, \alpha_2, \alpha_3, \cdots, \alpha_n] \quad (10)$$

where, n is the number of local maxima. From the envelop curve, the highest two peaks are identified and the time difference is calculated between them.

3.2.3. Interface region selection

The initial region for two interfaces are selected as the region where slopes are continuously decreasing. From the initial interface region, the exact interface region is selected by considering the ratio of highest signal amplitude in local maxima point and the signal amplitude of other local maxima points. If the ratio is greater than 0.5, than the region bound by those maxima point is the interface region. Then the corresponding signal is selected within that region of the local maxima to represent the interface echo.At this point we can calculate the thickness of each layer using Eq. (7)

3.2.4. Angle calculation

From the extracted region of interface echo, the phase angle is calculated from the coefficient of CWT in that region using the following equation

$$\theta_i = \tan^{-1}\frac{b_i}{a_i} \quad (11)$$

6

where, b_i is the imaginary component of the coefficient in i^{th} position of interface, and a_i is the real component of the coefficient in i^{th} position of interface.

3.2.5. Algorithm

Step 1: CWT with complex Gaussian function.

Step 2: Detect local maxima from the coefficient signal of CWT.

Step 3: Construct envelop curve using the signal amplitude in local maxima points.

Step 4: Find two highest peaks from the constructed signal.

Step 5: Select two interface region by calculating slope in both side of the peaks.

Step 6: Detect the highest local maxima in that region and discard the local maxima having the ratio greater than 0.5 with the highest local maxima.

Step 7: Find the coefficient value of the CWT signal within the region of the highest local maxima.

Step 8: Calculate time difference between two peaks to estimate thickness of each layer.

Step 9: Calculate the angle from the coefficient value to recognize the interface class.

4. Experimental setup and Results

Data have been analyzed in MATLAB software package, ver. 9.0.0 (R2016a) (The MathWorks, MA, U.S.A.). As shown in Fig. 8, the proposed methods were applied to a biological phantom which has three layers with the order of fat, muscle and fat. In the data measurement system shown in Fig. 1, with the temperature of the biological phantom set to 36° C, ultrasonic waves were irradiated in the direction of the arrow from the top of the 3-layer phantom to pass through the measurement points in the figure to obtain waveform data. The manual thickness measurement of each layer of the three-layer phantom was 8.1 mm for the first layer of fat, 7.4 mm for the first layer of muscle and 8.2 mm for the second fat layer. Ultrasonic measurement was performed four times using the three-layer phantom of Fig. 8, Measurement 1, which was the first measurement, acquired waveform is shown in Fig. 9. Our study utilized 4 measurements where each measurement consisted of 5 similar waveform acquired individually.

For template based method, threshold processing using standard deviation was performed to the measured waveform. The results are shown in Fig. 10. Through this process, we were able to identify the time when the ultrasonic wave reached the surface of the biological phantom, the time when the ultrasonic wave reached the bottom of
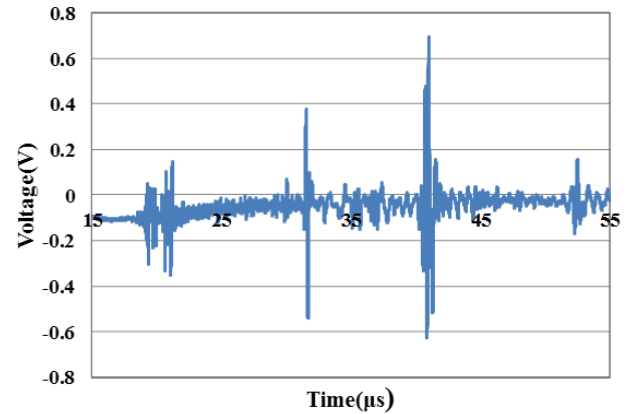

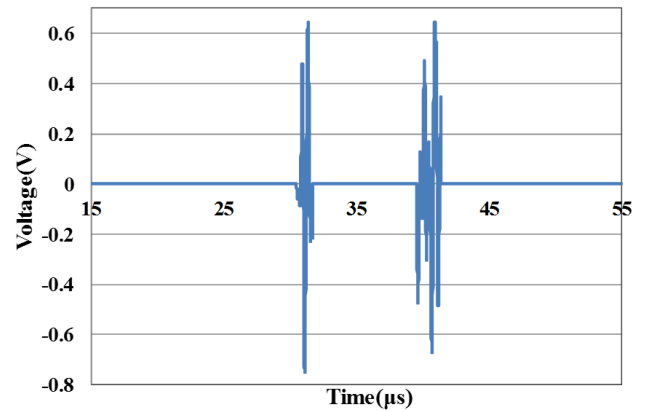Figure 9: Waveform acquisition of three-layer phantom

Figure 10: Results of narrowing the three-layer phantom interface

the three-layer phantom, and the fat-muscle interface candidate. Next, template matching using the templates of interface echo A and interface echo B, shown in Fig. 6, was applied to the identified boundary surface candidates. The result is shown in Fig. 11.

For CWT based method, we conducted CWT analysis using complex Gaussian wavelet. Fig. 12 gives the analysis result. The blue line is original signal, discrete signal at local maxima points are represented with purple line whereas green line gives CWT coefficients. After constructing wavelet the signal amplitude in local maxima points, two highest peaks from the new signal has been identified and slope in both side of the peaks are calculated to select the desired interface region.

In Fig. 12, interface region is represented by dotted lines. Next, we locate the highest local maxima in that region and discard the local maxima having the ratio greater than 0.5 with the highest local maxima. To see the phase difference between selected regions, angle from the coefficient value of the CWT signal within the region of the highest local maxima was calculated.
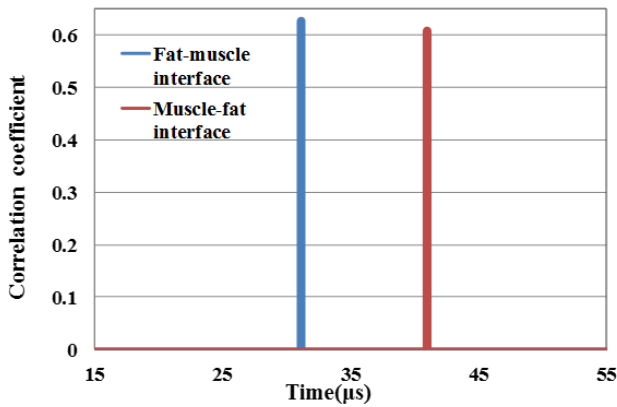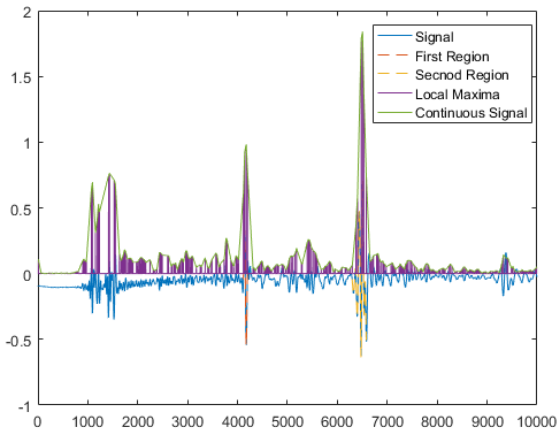
Figure 11: Template application result

Figure 12: Result of CWT based method. Blue line represents the Original signal, Purple line is Discrete signal at local maxima points, Green line shows CWT coefficients and Dotted line displays Interface region.

From Fig. 10, we can specify that the interface echo occurred at 4 points and can plot the time when ultrasonic wave reached to each boundary surface. For template based method, the propagation time of ultrasonic waves in each region was calculated by Eq. (6) and was multiplied by the sound velocity in the medium. The thickness of each region was calculated using Eq. (7). The results are shown in Table 1. For CWT based method, first the distance between two highest peaks of the signal constructed at step 4 was calculated. Next thickness of each layer was calculated using Eq. (7). Table 2 displays the result. For both methods, we calculated the absolute error between the truth value and estimated thickness. Table 3 and 4 show the comparison between the results of two methods and their mean absolute error.

Table 1: Thickness calculation results of each area of three-layer phantom using template based method

Measurement No.	Fat 1st layer (mm)	Muscle 1st layer (mm)	Fat 2nd layer (mm)
1	8.81	7.69	8.05
2	8.81	7.65	8.12
3	8.79	7.65	8.09
4	8.77	7.87	7.91

Table 2: Thickness calculation results of each area of three-layer phantom using CWT based method

Measurement No.	Fat 1st layer (mm)	Muscle 1st layer (mm)	Fat 2nd layer (mm)
1	7.79	7.30	8.01
2	7.55	7.33	8.30
3	7.65	7.45	8.27
4	8.06	7.42	8.15

5. Discussion

A study of muscle thickness measurement using a three-layer phantom of fat-muscle-fat has been introduced. Two separate methods have been proposed and compared from the viewpoint of measuring accuracy and flexibility. As a result, it was shown that the achievement of the CWT based method was better than the template based method. Furthermore, in the template based method, it is unnecessary to change the temperature during measurement, and it is possible to specify the medium in each region without comparing two or more waveforms. That is, the problem of the conventional temperature characteristics based method such as the difficulty of raising the temperature uniformly within the measurement range, or the measurement point is limited to one point, etc., was solved. But it was not flexible as we need to create template to locate the interface echo.

Table 3: Absolute error of each area of three-layer phantom using template based method

Measurement No.	Fat 1st layer (mm)	Muscle 1st layer (mm)	Fat 2nd layer (mm)
1	0.71	0.29	0.15
2	0.71	0.25	0.08
3	0.69	0.25	0.11
4	0.67	0.47	0.29
Mean	0.70	0.32	0.16

Table 4: Absolute error of each area of three-layer phantom using CWT based method

Measurement No.	Fat 1st layer (mm)	Muscle 1st layer (mm)	Fat 2nd layer (mm)
1	0.31	0.10	0.18
2	0.55	0.07	0.10
3	0.45	0.05	0.07
4	0.04	0.02	0.05
Mean	0.34	0.06	0.10

To overcome this problem, we introduced CWT based method which can automatically indicate the location of interface from the coefficient values. The number of layers need not be fixed like the first method, instead the method will work even if the nature of the signal is changed due to some factors like noise, density change etc, as use of standard deviation to select the region of interface might not perform well in noisy signal. In the second method we selected the region by calculating slope form the peak of highest local maxima point. So, it can find the region of interface with flexibility. For distance calculation only, this method will work for any type of signal.

6. Conclusion

In this study, we have proposed two muscle thickness measurement methods using 5.0 MHz ultrasonic single probe. By changing the order of medium of fat and muscle in the traveling direction of ultrasonic wave, interface echoes generated at the boundary surface can be confirmed to have a phase reversal phenomenon. Based on this characteristic, in the first method template of interface echo A was generated when the medium order is fat-muscle and interface echo B was generated when the medium order is muscle-fat, then the medium is identified by matching the templates. Also at the interface, it was revealed whether the divided medium was fat or muscle. For the second method, we used coefficient values of CWT analysis to select the interface region instead of template creation. The CWT time-frequency method employing the complex Gaussian wavelet was used to determine the instantaneous amplitude and frequency characteristics of the signals.

In an experimental environment, the proposed methods were applied to a fat-muscle-fat three-layer phantom. In the template based measurement of the three-layer phantom, the mean absolute error of the thickness was 0.32 mm, whereas for CWT based method showed 0.06 mm. It was observed that the level of the measurement precision is better in the CWT based method. The proposed methods addressed the problem of conventional temperature characteristics based method from the viewpoint of versatility and proved their feasibility as both does not require complicated temperature adjustment, and fixation of

measurement points, which was necessary for the conventional methods.

References

[1] B. H. Goodpaster, S. W. Park, T. B. Harris, S. B. Kritchevsky, M. Nevitt, A. V. Schwartz, E. M. Simonsick, F. A. Tylavsky, M. Visser, and A. B. Newman, The Loss of Skeletal Muscle Strength, Mass, and Quality in Older Adults: The Health, Aging and Body Composition Study, Journal of Gerontology: Medical Sciences, 61A (10) (2006), 1059-1064.

[2] S. W. Park, B. H. Goodpaster, E. S. Strotmeyer, L. H. kuller, R. Broudeau, C. Kammerer, N de Rekeneire, T. B. Harris, A. V. Schwartz, F. A. Tylavsky, Y. W. Cho, and A. B. Newman, Accelerated Loss of Skeletal Muscle Strength in Older Adults With Type2 Diabetes, The Health, Aging, and Body Composition Study, Diabetes Care, 30 (6) (2007).

[3] H. Hata, K. Kuramoto, S. Kobashi, and Y. Hata, Ultrasonic Muscular Thickness Determination by Temperature Rise, in: Proceeding of International Conference on Soft Computing and Intelligent Systems and the 14th International Symposium on Advanced Intelligent Systems, (2013).

[4] H. Horinaka, D. Sakurai, H. Sano, Y. Ohara, Y. Maeda, K. Wada, and T. Matsunaka, Optically Assisted Ultrasonic Velocity Change Images of Visceral Fat in a Living Animal, in: Proceeding of IEEE Ultrasonics Symposium, 2010, 1416-1419.

[5] N. Lamberti, L. Ardia, D. Albanese, and M. Di Matteo, An Ultrasound Technique for Monitoring the Alcoholic Wine Fermentation, Ultrasonics, 49 (2009), 94-97.

[6] S.E. Forrester and M.T.G. Pain, A Combined Muscle Model and Wavelet Approach to Interpreting the Surface EMG Signals from Maximal Dynamic Knee Extensions, Journal of Applied Biomechanics, 26 (2010), 62-72.

[7] L. Wang , C. Wang, F. Fu , X. Yu, H. Guo , C. Xu , X. Jing , H. Zhang , and X. Dong, Temporal Lobe Seizure Prediction Based on a Complex Gaussian Wavelet, Clinical Neurophysiology, (2011), 656-663.

[8] S. Jaffard, Y. Meyer and RD. Ryan, Wavelets Tools for Science and Technology, Society of industrial and Applied mathematics, Philadelphia, (2001).

[9] S. Furukawa, S. Kobashi, N. Kamiura, Y. Hata, S. Imawaki,and T. Ishikawa, Continuous-wavelet-transform-based Visualization for Seminiferous Tubule Using Broadband Ultrasonic Imaging, International Journal of Applied Electromagnetics and Mechanics, 52(1-2) (2016), 461-469.

[10] T. Bassani, and J. C. Nievola, Pattern Recognition for Brain-Computer Interface on Disabled Subjects using a Wavelet Transformation, Computational Intelligence in Bioinformatics and Computational Biology, (2008), 15-17.

[11] D. R. Wagner, Ultrasound as a Tool to Assess Body Fat, Journal of Obesity, (2013).